Applied Materials Today 38 (2024) 102221

Contents lists available at ScienceDirect

Applied Materials Today

journal homepage: www.elsevier.com/locate/apmt

An innovative approach for the passive cooling of batteries: An empirical investigation of copper deposition on polyurethane foam for the enhancement of phase change material

Keith M. Alcock *, Neil Shearer, Francisco Vedreño Santos, Zuansi Cai, Keng Goh

School of Computing, Engineering & the Built Environment, Edinburgh Napier University, UK

ARTICLE INFO

Keywords:
Battery
Phase change material
Passive thermal management
Copper
Polyurethane
Foam

ABSTRACT

A proof-of-concept utilising Copper-Plated Polyurethane Foam (CPPF) and Phase Change Material (PCM) for passive thermal management of lithium-ion batteries is demonstrated in this study. The aim of this research is to assess the effectiveness of CPPF when utilised as a constituent substance in PCM/Foam composites. Six distinct configurations of PCM/Foam composites are presented in this work using 10-pore-per-inch foam. A total of four deposition foam samples were produced. Of these, three were created by gradually increasing the immersion time in an electroless copper plating solution. For the fourth sample, an electroless plating technique was utilised for 80 min, followed by an electroplating procedure to deposit an additional layer of copper. The evaluation entails examining each plated sample in comparison to a copper foam that is commercially available with a purity level of 99.99 %. The findings reveal that the electroless-plated specimens exhibit improved effectiveness after being subjected to a prolonged plating period of 80 min. The electroplated sample exhibited the greatest degree of effectiveness, as evidenced by a 64.4 % reduction in battery cell surface temperature(10.98 °C), which is almost identical to the 64.5 % decrease in temperature (11.03 °C) observed with commercial foam but coupled with 88.1 % decrease in mass. The results suggest that the CPPF-PCM composites offer effective passive cooling properties for batteries.

1. Introduction

The successful integration of electrification and widespread use of renewable energy-technologies are necessary to form a low-carbon energy sector. Nevertheless, the escalating prevalence of electrification and the intrinsic unpredictability of renewable energy sources (e.g., solar and wind) pose obstacles to the stability of the power infrastructure and the guarantee of a dependable energy supply. Projections indicate that the worldwide power supply is anticipated to be predominantly derived from large-scale and high-capacity renewable energy production units by the year 2050, contributing around 86 % of the total [1]. Notably, solar photovoltaic and wind sources are expected to constitute a significant portion, accounting for approximately 58 % of the renewable energy generation [1].

Significant focus is presently devoted to the development of effective electrical energy storage devices in order to mitigate the inherent constraints of power grids, especially due to the unpredictable nature of renewable energy supply [2]. Moreover, the utilisation of fossil fuels in the context of transportation is responsible for approximately 14 % of global anthropogenic greenhouse gas emissions [3]. As a result, there is a growing tendency to shift away from transport modes with a large carbon impact [4]. The sales of electric vehicles had a substantial growth in 2017, exhibiting a noteworthy increase from 0.74 million units in the preceding year to 1.1 million units, denoting a huge rise of 51 % [5]. In 2022, the proportion of electric cars among all new car sales increased to 14 %, compared to around 9 % in 2021[6]. Additionally, electric car sales in Europe, the second largest market, experienced a growth rate of over 15 %, resulting in more than 20 % of all cars sold being electric and

Abbreviations: Cu-EP, electroplated copper; Cu-P, electroless plated copper; Cu-S, solid copper; CPPF, copper plated polyurethane foam; $CuSO_4$, $5H_2O$; CPPF-PCM, copper plater polyurethane foam phase change material; EDTA, ethylenediaminetetraacetic acid; KOH, potassium hydroxide; LIB, lithium-ion battery; LiPo, lithium polymer battery; NaOH, sodium hydroxide; $NaPO_2H_2{\cdot}H_2O$, sodium hypophosphite monohydrate; PCM, phase change material; PUF, polyurethane foam; SEM, scanning electron microscope; TC, thermocouple; T_{start}, discharge starting temperature (°C); 2-MBT, 2-Mercaptobenzothiazole.

* Corresponding author.
E-mail address: keith.alcock@napier.ac.uk (K.M. Alcock).

https://doi.org/10.1016/j.apmt.2024.102221
Received 15 February 2024; Received in revised form 15 April 2024; Accepted 29 April 2024
Available online 4 May 2024

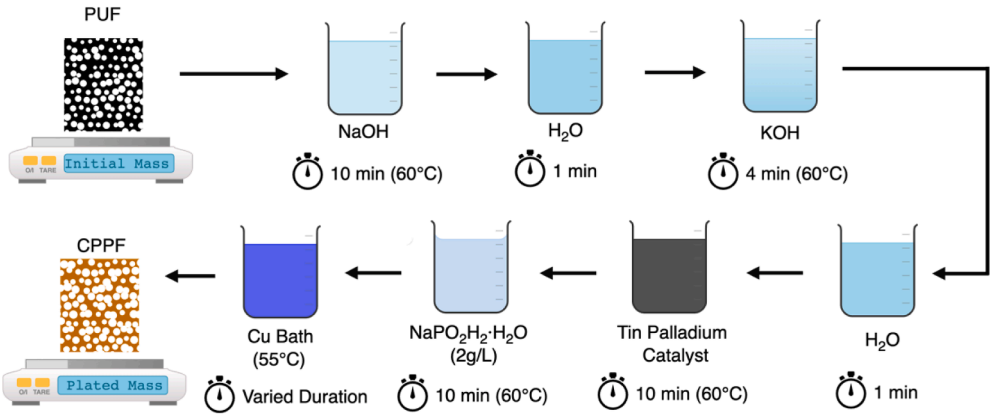

Fig. 1. Process for the electroless deposition on PU foam, where the foam sample is weighed before and after the deposition process.

in the United States, which is the third biggest market a significant growth of 55 % was seen, resulting in a sales share of 8 % [6].This signifies a significant shift towards more environmentally friendly transportation options.

The accelerating deployment and development of battery technologies is expected to result in lithium-based batteries assuming a more prominent role over a wider range of capacities, ranging from the use of grid scale storage to electric vehicles, thus, the temperature monitoring and management is a crucial aspect in mitigating degradation and enhancing longevity of lithium-based batteries, which is well-established in the literature [3,7–11]. The optimisation of temperature gradients is advantageous for ensuring the safety and durability of Lithium-Ion Batteries (LIBs), making the battery thermal management system a pivotal component in attaining adequate temperature regulation [12]. Lithium batteries can experience a decrease in charge efficiency and reduced lifetime when exposed to temperatures over 50 °C [13]. Consequently, industrial setting, especially in electric vehicles, commonly employ forced air or indirect liquid cooling methods [14].

The adoption of Phase Change Material (PCM) is becoming more widespread particularly with the ongoing development of passive thermal management systems [14]. A PCM is a substance that undergoes a transition between solid and liquid phases, known as a melt-solidification cycle, during which it absorbs energy from the surrounding environment, while maintaining a relatively constant temperature [15,16]. The utilisation of PCM in battery applications has been extensively documented in academic research works. These studies have thoroughly examined the employment of PCMs both independently and in conjunction with liquid and air active cooling systems to regulate the operating temperatures of batteries [17–24]. The internal temperature control of LIB cells has also found use for PCM as a battery separator component [25].

Due to the inherent low thermal conductivity of PCMs [26–28], foams are finding increased utilisation of the enhancement of PCM thermal capacity [29]. Foams are a porous structure known for their unique physical and mechanical qualities, which find widespread use in various applications, including energy and blast resistance, fire resistance, thermal insulation, vibration, and sound dampening, as well as lightweight applications such as foam core sandwich panels [30,31]. The use of foam structures in passive thermal methodologies to enhance the thermal conductivity of PCMs is an emerging technology, where the PCM is infiltrated into the porous foam materials creating a composite [27,32,33]. The fabrication of PCM/foam composites typically use copper, nickel, or aluminium foam as main components to enhance the heat transfer into the PCM due to the high thermal conductivity of these metals and interconnecting three-dimensional structure [27,34–38].

Despite the significant enhancement they provide to the performance of phase change materials, metal foams are currently not commercially viable due to their high cost [28,39,40]. Furthermore, due to the fact that metal foams are made from dense materials such as copper, it becomes challenging to endorse the use of PCM composites including these component parts for applications which are weight sensitive. As a result, there is potential to utilise the low-cost [41] and lightweight [42] properties of polymer foams, which have been largely overlooked in existing research. There are a small selection of works, notably, in [43] the plating of pure nickel is investigated for the coating of urethane-based structures for battery-related components, although not for PCM enhancement, and in [44] a dense melamine foam was utilised as a structure for carboxy-rich carbon and boron nitride and infiltrated with polyethylene glycol phase change material, aimed at addressing the rigidity and low light absorption issues for solar applications.

The available literature lacks academic publications on the compositions and usage of plated polymer foam in phase change materials, which is in contrast to the extensive research on solid metal foams for passive thermal management of batteries. This indicates a clear gap in the field. This gap presents an opportunity to explore the intersection between the use of lightweight polymer foams and the heat conductivity characteristics displayed by metals. The successful advancement of these composites has the capacity to greatly impact passive heat management systems that utilise PCM. This is especially crucial in applications where weight is a vital factor, such as electric vehicles and aircraft. The primary objective of this work is to examine the efficacy of composites consisting of Copper Plated Polyurethane Foam and Phase Change Material (CPPF-PCM) in enhancing the passive heat regulation of lithium-based batteries, while utilising reduced mass compared to solid metal foam. Given that prior studies have extensively utilised metal foam materials, the foams produced in this study are therefore subject to a comparative analysis with a commercially available copper foam that has a purity level of 99.99 %. This study conducts an empirical investigation to assess the practicality of using CPPF-PCM composites as a means of passively cooling batteries. It aims to fill a significant gap in the current body of research and has the potential to provide valuable knowledge in the field of battery thermal management, particularly in relation to emerging PCM/foam composites.

2. Materials & methods

2.1. Foam/PCM composite

This work investigates six distinct arrangements of PCM/foam composites, employing a foam structure characterised by a consistent pore density of 10 pores per inch across all combinations. The chosen pore density was based on its prevalence in research using PCM [29,34], furthermore, a pore per inch density of 10 indicates a larger pore size, which facilitates the infiltration of PCM into the structure. The composite materials comprise an initial component of Polyurethane Foam (PUF) with a reported thermal conductivity range of 0.018∼0.032 W/m.

Table 1
Cu Plating Bath Constituents.

Component	*Concentration(g/L)*
$CuSO_4 \bullet 5H_2O$	*20*
Ethylenediaminetetraacetic acid (EDTA)	*40*
Glyoxylic Acid (50% wt in H_2O)	*10.5*
2-mercaptobenzothiozole *(2MBT)*	*0.002*

Bath Temperature = 55 °C, pH 12–12.5 - All chemicals sourced from Sigma Aldrich, UK.

K [45], along with four alternate variants that use plating processes on the PUF, as well as a commercially available foam. A 'green' electroless plating approach is utilised for the four copper-plated variants, and one of these electroless samples is further altered with an additional electroplating process. A commercially available copper foam is employed as a benchmark for evaluating the effectiveness of the plated substitutes. This section will assess the techniques employed in the fabrication of PCM/foam composites and the protocol for testing.

2.1.1. Copper deposition methodology

The electroless copper plating technique is mostly based on the approach presented in [46,47], with the exception of the inclusion of chitosan. However, the approach presented in this paper integrates the use of 2-mercaptobenzothiozole (2-MBT) as a stabilising agent, as suggested in [48], this stabilises the bath against the formation of undesired cuprous particles, and the optimum concentration of 2 mg/L is utilised. The substrate preparation adheres to the prescribed methodology outlined in [47]. The overall process is displayed in Fig. 1. The inclusion of 2-MBT enables the plating bath to maintain its functionality for a duration of 80 min, despite the absence of aerated agitation. Instead of the conventional use of formaldehyde, this process adopts an environmentally friendly approach by employing glyoxylic acid as a reducing agent. The chemical concentrations utilised in the plating process are outlined in Table 1. In order to provide consistent and uniform heating of the copper bath solution, a Heidolph MR Hei-Standard hotplate with a Heidolph 1 litre oil bath adapter is utilised. This oil bath accommodates the beaker containing the copper plating bath, to provide uniform heating throughout the deposition process.

A series of four deposition foam samples were generated, with the initial three samples produced by a progressive increase of immersion duration in the copper plating solution, starting at 20 min, then advancing to 40 min, and finally reaching 80 min. To add an extra layer of copper, the electroplating technique is applied on the fourth sample, specifically, a sample with an electroless plating length of 80 min. The electrolyte solution employed in the electroplating process comprises two main inorganic constituents: copper sulphate pentahydrate (200 g/L) serves as the source of copper ions, while sulfuric acid (45 g/L) enhances the solution's conductivity and serves as a charge carrier [49]. The electroplating procedure was carried out under a current of 1A and a voltage of 4 V. Both sides of the foam structure were exposed for a duration of 10 min, resulting in a total plating time of 20 min, and ensuring a more even plating throughout the porous structure.

Henceforth, the plated foam samples will be denoted as Cu-P 20, Cu-P 40, Cu-P 80, and Cu-EP. The acronym Cu-P refers to the electroless plating method, where the numerical number appended indicates the length of time immersed in the copper bath. Conversely, the abbreviation "EP" denotes the electroplating process. In addition, the abbreviation PUF is used to refer to the plain polyurethane foam, whereas Cu-S is used to identify the commercially available foam. Fig. 2(a) and (b) illustrate examples of the samples Cu-S and Cu-P 20, respectively. Additionally, Fig. 2(c), (d), and (e) depict the foam after 20, 40, and 80-minute plating processes, respectively, clearly showing the existence of a visible copper layer on the foam structure which appears to be more consistent as the deposition time increases.

2.1.2. PCM selection

The PCM/foam composites utilise commercial phase change material sourced from Rubitherm Technologies GmbH, namely RT31. The discharge of the EEMB LP963450 Lithium Polymer (LiPo) battery cell starts at ~25 °C and terminates at ~42 °C when discharged at 1.5 C, as seen in Fig. 3(a). To effectively absorb the heat generated by the cell, the PCM must operate within this specified temperature range. According to the manufacturer's specifications, the solid to liquid transition range of the RT31 PCM is reported to be between 29 °C and 34 °C, with a main peak observed at 31 °C, and obtains a thermal conductivity of 0.2 W/m. K. The heat absorption of the RT31 PCM was measured using a TA Instruments Q2000 Differential Scanning Calorimeter, the transition onset temperature of the PCM is observed to be 24.92 °C, while the peak transition temperature is measured at 32.32 °C (Fig. 3(b)). This suggests that the phase change material PCM is very suitable for the intended use, especially considering that the experimental setup employed a constant

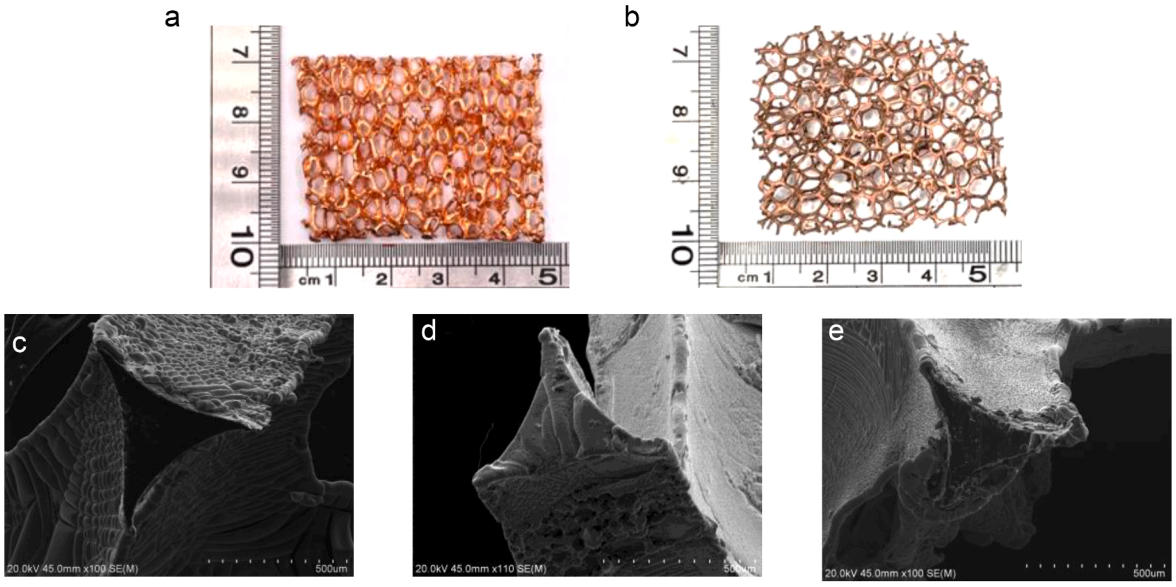

Fig. 2. Visual representation of Foam, (a) commercial 10PPI foam (Cu-S), (b) example of Cu-P 20 foam, (c) SEM imaging of 20-minute deposition, showing foam strut end, (d) SEM image of strut end of 40-minute electroless plating, and (e) SEM image of foam strut end after 80 min in electroless bath.

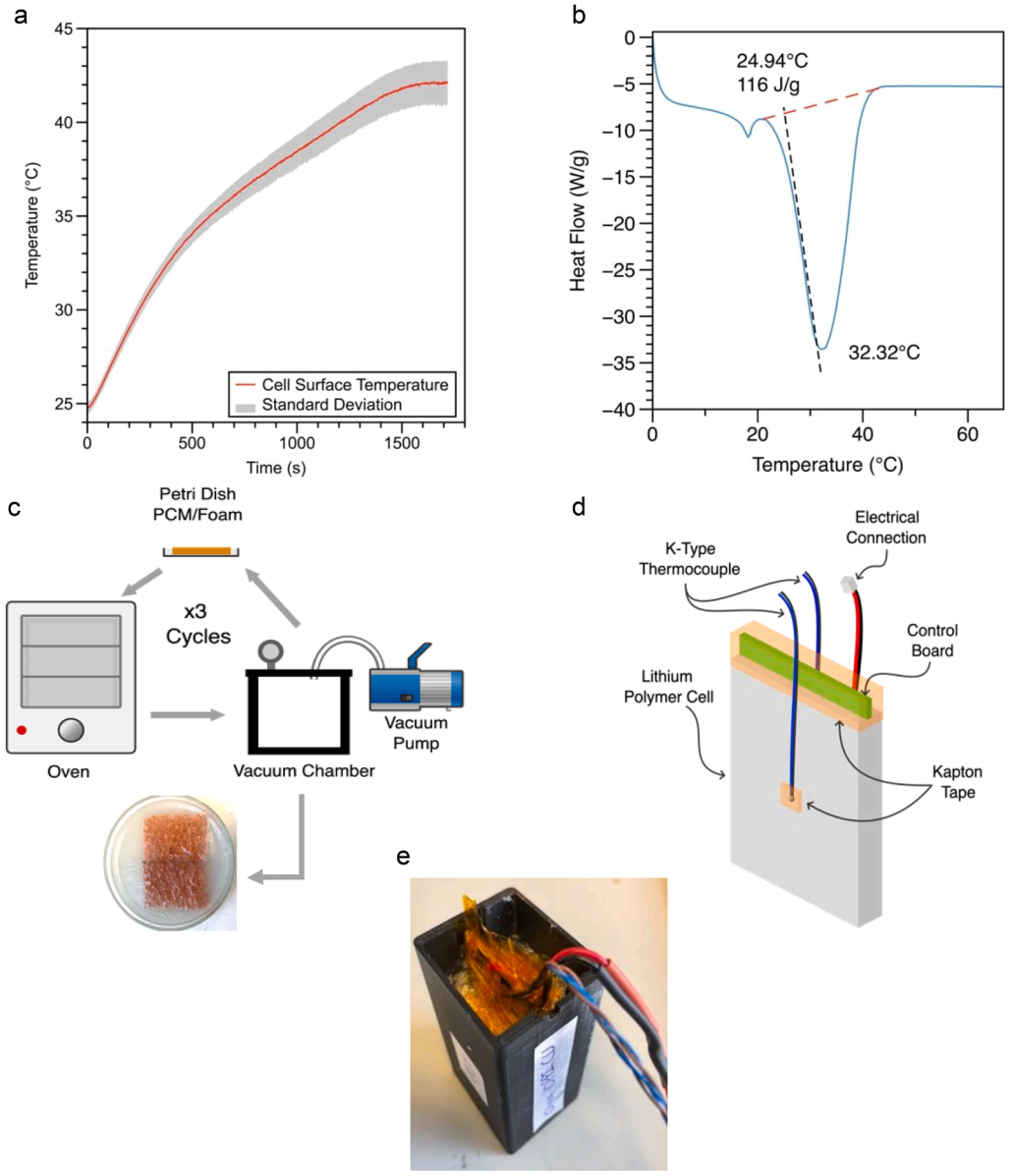

Fig. 3. Experimental Materials and Method; (a) Cell surface temperature change at 1.5C, three test average, displaying standard deviaiton, (b) solid to liquid transition phase of RT31 PCM, (c) illustration of PCM infiltration method with example of infiltratrated copper foam, (d) illustrated example of the lithium polymer cell with K-Type thermocouple placement, and (e) image of fully assembly for testing. .

temperature chamber maintained at 25 °C ± 1 °C, as elaborated upon in Section 2.2 Experimental Setup.

The proximity of the onset transition temperature to the discharge start temperature (T_{start}), as well as the fact that the transition peak temperature is lower than the expected final temperature of the cell after discharge, enables the PCM to fully utilise its capacity. Consequently, this facilitates the evaluation of the foams for the thermal management of the chosen battery cell.

2.1.3. PCM infiltration

The foam substrates undergo a vacuum infiltration with PCM, as seen in Fig. 3(c). This procedure has a resemblance to the approach described in other works [12,50–52]. The foam samples are carefully arranged within a glass Petrie dish, which is subsequently filled with liquid PCM. The Petrie dish is then introduced into the vacuum chamber, and the vacuum environment is sustained until the PCM visibly solidifies. Following this, the Petrie dish is placed into a Binder FD23 oven set at 45 °C, maintaining this temperature for 30 min to facilitate the transition of the PCM from its liquid to a solid state. To achieve thorough infiltration of the PCM into the foam structure, the process is repeated three times. Once a state of stable low pressure is reached within the vacuum chamber, the expulsion of air from the foam material becomes evident, manifesting as visible bubbles on liquid PCM's surface. These phenomena aid the infiltration of the phase change material into the porous structure of the foam.

To quantify the extent of PCM infiltration into the foam structure, a dimensionless parameter known as the impregnation ratio (α) is calculated using (1). This parameter serves as a metric for evaluating the compatibility between the foam and PCM, with a value of 1 indicating optimal PCM penetration into the foam structure [12].

$$\alpha = \frac{\Delta m_i}{\varepsilon_b V_t \rho_{pcm}} \tag{1}$$

$$\varepsilon_b = \frac{m_{fo}}{\rho_{sk} V_t} \tag{2}$$

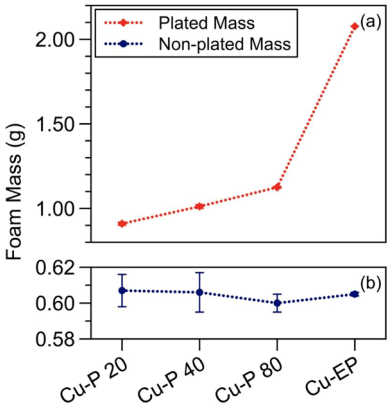

Fig. 4. (a) foam mass after Cu deposition, and (b) foam mass before Cu depostion. All showing average of three measurments, error bars displaying standard deviaiton. .

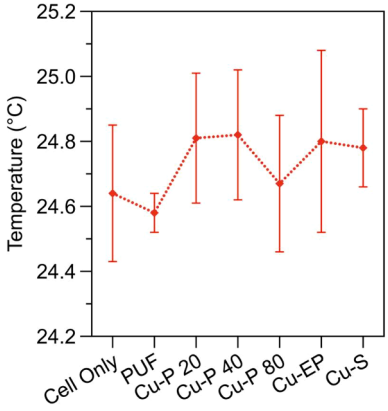

Fig. 5. Average T_{start} of each discharge test. All showing average of three tests, error bars displaying standard deviaiton.

Where Δm_i is the mass difference between the PCM/foam composite and that of the foam itself, ρ_{pcm} is the density of the PCM in solid phase, V_t is the total volume of the foam piece and ε_b is the bulk porosity which is defined in (2) [12].

Where, m_{fo} is the mass of the foam piece and ρ_{sk} is the density of the foam skeleton. This ratio is found to be in the range of 0.937 and 0.983, suggesting excellent PCM infiltration into the foam skeleton.

2.2. Experimental setup

The surface temperature of the battery cell is measured by attaching pre-calibrated k-type thermocouples (LABFACILITY, obtained from Farnell, UK) to the surface using Micro-Measurements M-Bond 200 adhesive. These thermocouples conform to the IEC 584–2 class 1 standard. To enhance their stability and protect them from external factors, a thin layer of polyimide (Kapton®) tape is applied over the thermocouples, as seen in Fig. 3(d).

The PCM foam composites are housed in a specially designed casing manufactured through 3D printing techniques (Fig. 3(e)). The design of the container accommodates PCM/Foam composites with an optimal uniform thickness of 10 mm on either side of the LiPo cell [20]. The PCM foam composites that have been infiltrated are positioned between the surface of the cell and the wall of the casing. The casing is intentionally designed with an increased height, considering the 12.5 % expansion coefficient, to prevent liquid overflow during the phase transition.

The LiPo cell undergoes charging using a B&K Precision 9202 DC power supply at a rate of 0.5 C until the desired cut-off current of 36 mA is achieved. Prior to discharging using a B&K Precision 8601 DC electronic load, the sample under examination undergoes a rest period within an ESPEC LU114 constant temperature chamber until the temperature readings from both TC sensors reach a state of thermal equilibrium of ~25 °C. To ensure data consistency for comparative analysis, all discharge tests are conducted within the constant temperature chamber. The acquisition of thermocouple data from the surface of the LiPo cell is facilitated by the utilisation of a Pico Technology TC-08 thermocouple data recorder and Picolog software. The cells undergo discharge using a B&K Precision 8601 DC electronic load at a rate of 1.5 C. All data is obtained at a frequency of 1 Hz.

3. Results & discussion

3.1. Foam mass and Cu deposition

A linear connection between the time of immersion in the Cu bath and the mass of the foam is seen based on the measurements conducted of the foam's mass before and after each plating session, as depicted in Fig. 4(a). The experimental results show that when the deposition period rises from 20 min to 40 and 80 min, the average mass of Cu applied also increases from 0.910 g to 1.012 g and 1.125 g, respectively. Furthermore, it is important to notice that the electroplating process results in a significant mass increase for the foam.

The electroless deposition method demonstrates a lower rate of mass growth in comparison to electroplating, primarily due to the differences in their respective processes. The electroplating process involves using a copper token that is 99.99 % pure and weighs 17.90 g. This token can be utilised until it is completely used up, ensuring that there remains sufficient copper available for deposition. However, the electroless approach depends on the amount of copper in the plating solution, which is incorporated using copper sulphate pentahydrate, as depicted in Table 1. As the duration of plating progresses, the rate of plating decreases as the limited amount of copper in the bath is being utilised. Furthermore, a high concentration of glyoxylic acid was used at a relatively high temperature, which, without a stabiliser, will decompose rapidly. This decomposition leads to the formation of copper deposits in the bath solution, causing a decrease in chemical concentration [47]. As mentioned previously, the purpose of adding 2-MBT as a stabiliser was to increase the longevity of the plating bath and minimise its decomposition. However, it is noteworthy that there are some copper deposits found at the bottom of the beaker used for the plating bath at the end of each plating period. As a result, the copper formation and mass on the PUF is anticipated to be lower in the electroless process compared to electroplating. It is crucial to highlight that the electroless process is essential for producing the Cu-EP sample since it provides the electrically conductive copper layer necessary for initiating the electroplating mechanisms.

As anticipated, the plated samples demonstrate a significant reduction in mass compared to the mass of the Cu-S foam, which was measured as 17.40 g. The experimental findings suggest that the Cu-P 20, 40, 80, and Cu-EP foam samples have a mass difference of −94.8 %, −94.2 %, −93.5 %, and −88.1 %, respectively, in comparison to the Cu-S foam. It is crucial to note the foam's mass prior to plating, as this parameter serves as a key factor in determining the mass of the thermally conductive copper layer on the foam.

The average mass of the PUF substrate before plating exhibits a constant range of 0.60 g to 0.62 g, as seen in Fig. 4(b). The consistency across values ensures a dependable basis for evaluating the copper deposition layer, enabling accurate assessment and comparison throughout the plating process.

3.2. Foam effect on cell temperature

The initial temperature, denoted as T_{start}, is crucial for the effectiveness of each experiment since it directly affects the end temperature

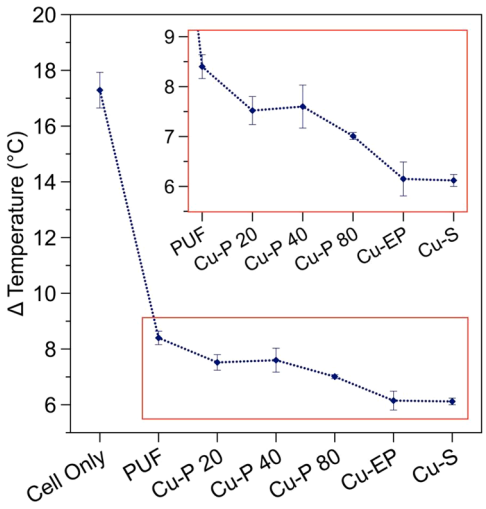

Fig. 6. The average ΔT of LiPo cell surface at the after 1.5C discharge. Showing the average of three tests, error bars displaying standard deviaiton. .

of the LiPo battery. The T_{start} is set at 25 °C, as observed in past studies using lithium-ion batteries [3]. Shown in Fig. 5, the temperature measured before the discharge begins varies between 24.43 °C and 25.08 °C. The ESPEC LU114 chamber used in the testing process maintains the ambient temperature with a tolerance of ±1 °C. To ensure correct assessment of the PCM/foam composites, it is crucial to maintain a consistent initial temperature and ambient temperature throughout the process, since this allows for precise comparison of the final cell temperatures. The temperature change, ΔT, of the LiPo cell due to the discharge is shown in Fig. 6 for all samples. In the absence of any passive cooling mechanism, the cell undergoes an average surface temperature increase of 17.3 °C, reaching a maximum temperature of 42 °C. When using only the PUF material in PCM, the average surface temperature reaches 33 °C, with a temperature difference (ΔT) of 8.40 °C. This demonstrates a substantial decrease of 51.4 % in temperature compared to the cell that does not employ passive cooling. This is linked to the implementation of the PCM. By incorporating the PUF into this specific sample, the evaluation of the coated foam samples and the resulting temperature reduction at the cell surface can be achieved.

The copper electroless plating contributes to a subsequent reduction, amounting to 56.5 %, 56.1 %, and 59.4 % lower temperatures for Cu-P 20, Cu-P 40, and Cu-P 80, respectively, compared to the cell alone. Furthermore, an analysis of the samples Cu-P 20 and Cu-P 40, reveals that the plating duration and the increase in copper do not significantly reduce the temperature. The comparison of Cu-P 80, Cu-P 40, and Cu-P 20 reveals a minimal improvement of 3.4 % and 3 % correspondingly. The Cu-P 20 sample shows a slightly superior outcome compared to the Cu-P 40 sample, with a difference of −0.4 %. This can be attributed to challenges in accurately controlling the plating solution with glyoxylic acid as the reducing agent, as it is sensitive to temperature [47]. Therefore, minor temperature changes in the plating bath could lead to unknown variations in deposition rates. Based on the evidence shown in Fig. 6, it is recommended that the optimal length for plating is 80 min. This conclusion is further supported by the data displayed in Fig. 7(a). Moreover, when comparing the three different durations of electroless deposition, there is a discernible variation in the results' standard deviation (represented by error bars in Fig. 7(a)) for both the Cu-P 20 and Cu-P 40 samples, indicating an inconsistent plating process.

Fig. 7(b) depicts the performance of the Cu-P 80 sample in relation to the Cu-EP and Cu-S samples. Results indicate a notable reduction in the temperature change, with the Cu-S sample exploiting the commercially available copper foam demonstrating the highest degree of effectiveness. Nevertheless, the Cu-EP sample has a marginally greater ΔT, albeit the increase is only 0.2 °C. This finding presents clear evidence that the Cu-EP sample has similar performance to the commercially available foam, despite the latter possessing a substantially greater copper mass, 88.1 % more. In terms of performance, the Cu-P 80 sample demonstrated a reduction in cell temperature of 59.4 % compared to the LiPo cell alone. Furthermore, the Cu-EP and Cu-S samples exhibited reductions of 64.4 % (overall reduction of 10.98 °C) and 64.5 % (overall reduction of 11.03 °C) respectively.

4. Conclusions

This study proposes a novel research direction that involves analysing the weight considerations of PCM/foam composites and emphasising the significance of material quantity as a crucial parameter for successful passive cooling approaches. The findings presented in this study demonstrate the first experimental investigation of copper deposition on polymer foam as a means of achieving passive temperature regulation in battery systems. The evaluation of different cooling strategies relies on analysing the fluctuation in surface temperature of a LiPo cell during a discharge at a rate of 1.5C. It has been shown that in the absence of any cooling mechanism, the LiPo cell experiences an average increase in surface temperature of 17.3 °C.

The plating deposition process, conducted for durations of 20, 40, and 80 min results in temperature reductions of 56.5 %, 56.1 %, and 59.4 %, respectively, when compared to the control cell without cooling. The effectiveness of the electroless-plated samples increases with an extended plating duration of 80 min. The Cu-EP variant, with an

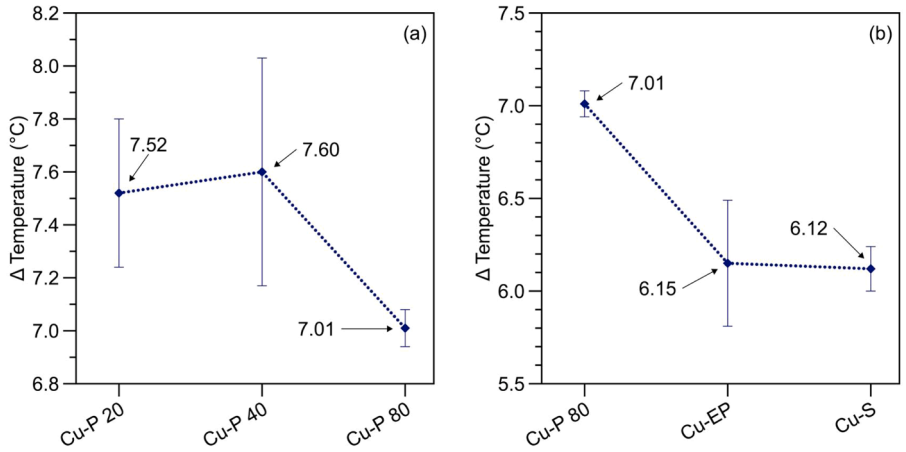

Fig. 7. The average ΔT of LiPo cell surface at the after 1.5C discharge, (a) of the Cu-P durations, and (b) showing Cu-P 80, Cu-EP and Cu-S samples. All showing the average of three tests, error bars displaying standard deviation. .

additional electroplated layer, demonstrates the highest degree of effectiveness, as indicated by an average decrease in cell surface temperature of 64.4 %. This reduction is nearly identical to the 64.5 % observed with the Cu-S arrangement. The Cu-EP sample demonstrates a significant decrease in mass, 88.1 % in comparison to the Cu-S sample. This finding suggests that the current study offers empirical support for the benefits of utilising copper deposition on polyurethane foams to improve passive thermal management strategies involving phase change materials. In its conclusion, this proof-of-concept study highlights the advantages this novel material and warrants the undertaking additional research in this area. It will be essential to conduct additional research on the effectiveness of the plating bath and establish an approach of scaling up the process for commercial use.

CRediT authorship contribution statement

Keith M. Alcock: Conceptualization, Investigation, Writing – original draft, Writing – review & editing, Visualization. **Neil Shearer:** Writing – review & editing, Resources, Conceptualization. **Francisco Vedreño Santos:** Writing – review & editing, Supervision. **Zuansi Cai:** Writing – review & editing, Supervision. **Keng Goh:** Writing – review & editing, Supervision, Project administration, Funding acquisition, Conceptualization.

Declaration of competing interest

The authors declare that they have no known competing financial interests or personal relationships that could have appeared to influence the work reported in this paper.

Data availability

Data will be made available on request.

References

[1] Z. Zhu, et al., Rechargeable batteries for grid scale energy storage, Chem. Rev. 122 (22) (2022) 16610–16751, https://doi.org/10.1021/acs.chemrev.2c00289, 2022/11/23.

[2] X. Luo, J. Wang, M. Dooner, J. Clarke, Overview of current development in electrical energy storage technologies and the application potential in power system operation, Appl. Energ. 137 (2015) 511–536, https://doi.org/10.1016/j.apenergy.2014.09.081, 2015/01/01/.

[3] K.M. Alcock, M. Grammel, Á. González-Vila, L. Binetti, K. Goh, L.S.M. Alwis, An accessible method of embedding fibre optic sensors on lithium-ion battery surface for in-situ thermal monitoring, Sens. Actuators A 332 (2021), https://doi.org/10.1016/j.sna.2021.113061.

[4] F.Y. Fu, et al., The dynamic role of energy security, energy equity and environmental sustainability in the dilemma of emission reduction and economic growth, J. Environ. Manage. 280 (2021) 111828, https://doi.org/10.1016/j.jenvman.2020.111828, 2021/02/15/.

[5] X.G. Yang, S. Ge, N. Wu, Y. Mao, F. Sun, C.Y. Wang, All-climate battery technology for electric vehicles: inching closer to the mainstream adoption of automated driving, Ieee Electrification Mag. 7 (1) (2019) 12–21, https://doi.org/10.1109/MELE.2018.2889545.

[6] I. E. A. (IEA), "Global EV Outlook 2023," 04/23 2023. [Online]. Available: https://www.iea.org/reports/global-ev-outlook-2023.

[7] J. Huang, S.T. Boles, J.-M. Tarascon, Sensing as the key to battery lifetime and sustainability, Nat. Sustain. 5 (3) (2022) 194–204, https://doi.org/10.1038/s41893-022-00859-y, 2022/03/01.

[8] E. McTurk, T. Amietszajew, J. Fleming, R. Bhagat, Thermo-electrochemical instrumentation of cylindrical Li-ion cells, J. Power Sources 379 (2018) 309–316, https://doi.org/10.1016/j.jpowsour.2018.01.060.

[9] J. Fleming, T. Amietszajew, E. McTurk, D. Greenwood, R. Bhagat, Development and evaluation of in-situ instrumentation for cylindrical Li-ion cells using fibre optic sensors, Hardwarex 3 (2018) 100–109, https://doi.org/10.1016/j.ohx.2018.04.001.

[10] K.M. Alcock, et al., Individual cell-level temperature monitoring of a lithium-ion battery pack, Sensors 23 (9) (2023), https://doi.org/10.3390/s23094306.

[11] K.M. Alcock, M. Grammel, L. Binetti, Á. González-Vila, K. Goh, L.S.M. Alwis, Feasibility study on the potential of Fibre Bragg gratings for thermal monitoring of cylindrical lithium-ion batteries, in: G.W.A.D.M. Cranch, P. Dragic (Eds.), Optical Fiber Sensors Conference 2020 Special Edition, Optical Society of America, Washington, DC, 2020, https://doi.org/10.1364/OFS.2020.T3.49, 2020/06/08in OSA Technical Digest, p. T3.49[Online]. Available: http://www.osapublishing.org/abstract.cfm?URI=OFS-2020-T3.49.

[12] X. Xiao, P. Zhang, M. Li, Preparation and thermal characterization of paraffin/metal foam composite phase change material, Appl. Energ. 112 (2013) 1357–1366, https://doi.org/10.1016/j.apenergy.2013.04.050, 2013/12/01/.

[13] N. Sato, Thermal behavior analysis of lithium-ion batteries for electric and hybrid vehicles, J. Power Sources 99 (1) (2001) 70–77, https://doi.org/10.1016/S0378-7753(01)00478-5, 2001/08/01/.

[14] G. Zhao, X. Wang, M. Negnevitsky, H. Zhang, A review of air-cooling battery thermal management systems for electric and hybrid electric vehicles, J. Power Sources 501 (2021) 230001, https://doi.org/10.1016/j.jpowsour.2021.230001, 2021/07/31/.

[15] A.S. Fleischer, *Thermal Energy Storage Using Phase Change Materials, Fundamentals and Applications* (SpringerBriefs in Applied Sciences and Technology), Springer International Publishing, 2015.

[16] S. Ushak, et al., A review on phase change materials employed in Li-ion batteries for thermal management systems, Appl. Mater. Today 37 (2024) 102021, https://doi.org/10.1016/j.apmt.2023.102021, 2024/04/01/.

[17] G.-H. Kim, J. Gonder, J. Lustbader, A. Pesaran, Thermal management of batteries in advanced vehicles using phase-change materials, World Electr. Veh. J. 2 (2) (2008), https://doi.org/10.3390/wevj2020134.

[18] X. Duan, G.F. Naterer, Heat transfer in phase change materials for thermal management of electric vehicle battery modules, Int. J. Heat Mass Transf. 53 (23) (2010) 5176–5182, https://doi.org/10.1016/j.ijheatmasstransfer.2010.07.044, 2010/11/01/.

[19] Z. Ling, F. Wang, X. Fang, X. Gao, Z. Zhang, A hybrid thermal management system for lithium ion batteries combining phase change materials with forced-air cooling, Appl. Energ. 148 (2015) 403–409, https://doi.org/10.1016/j.apenergy.2015.03.080, 2015/06/15/.

[20] J. Weng, X. Yang, G. Zhang, D. Ouyang, M. Chen, J. Wang, Optimization of the detailed factors in a phase-change-material module for battery thermal management, Int. J. Heat Mass Transf. 138 (2019) 126–134, https://doi.org/10.1016/j.ijheatmasstransfer.2019.04.050.

[21] G. Ye, G. Zhang, L. Jiang, X. Yang, Temperature control of battery modules through composite phase change materials with dual operating temperature regions, Chem. Eng. J. 449 (2022) 137733, https://doi.org/10.1016/j.cej.2022.137733, 2022/12/01/.

[22] Y. Lv, G. Liu, G. Zhang, X. Yang, A novel thermal management structure using serpentine phase change material coupled with forced air convection for cylindrical battery modules, J. Power Sources 468 (2020) 228398, https://doi.org/10.1016/j.jpowsour.2020.228398, 2020/08/31/.

[23] Y.A. Bhutto, A.K. Pandey, R. Saidur, K. Sharma, V.V. Tyagi, Critical insights and recent updates on passive battery thermal management system integrated with nano-enhanced phase change materials, Mater. Today Sustain. 23 (2023) 100443, https://doi.org/10.1016/j.mtsust.2023.100443, 2023/09/01/.

[24] Y. Lv, X. Yang, G. Zhang, Durability of phase-change-material module and its relieving effect on battery deterioration during long-term cycles, Appl. Therm. Eng. 179 (2020) 115747, https://doi.org/10.1016/j.applthermaleng.2020.115747, 2020/10/01/.

[25] Z. Liu, Q. Hu, S. Guo, L. Yu, X. Hu, Thermoregulating separators based on phase-change materials for safe lithium-ion batteries, Adv. Mater. 33 (15) (2021) 2008088, https://doi.org/10.1002/adma.202008088, 2021/04/01.

[26] R. Kothari, S.K. Sahu, S.I. Kundalwal, S.P. Sahoo, Experimental investigation of the effect of inclination angle on the performance of phase change material based finned heat sink, J. Energy Storage 37 (2021) 102462, https://doi.org/10.1016/j.est.2021.102462, 2021/05/01/.

[27] R. Kothari, S.K. Sahu, S.I. Kundalwal, P. Mahalkar, Thermal performance of phase change material–based heat sink for passive cooling of electronic components: an experimental study, Int. J. Energ. Res. 45 (4) (2021) 5939–5963, https://doi.org/10.1002/er.6215, 2021/03/25.

[28] G. Righetti, C. Zilio, K. Hooman, S. Mancin, Market-orientated solutions to increase thermal conductivity in latent thermal energy storage systems, Appl. Therm. Eng. 243 (2024) 122583, https://doi.org/10.1016/j.applthermaleng.2024.122583, 2024/04/15/.

[29] A. Diani, L. Rossetto, Melting of PCMs embedded in copper foams: an experimental study, Materials (Basel) 14 (5) (2021), https://doi.org/10.3390/ma14051195.

[30] M.D. Goel, V.A. Matsagar, S. Marburg, A.K. Gupta, Comparative performance of stiffened sandwich foam panels under impulsive loading, J. Performance Construct. Facilities 27 (5) (2013) 540–549, https://doi.org/10.1061/(ASCE)CF.1943-5509.000034.

[31] A. Kulshreshtha, S.K. Dhakad, Preparation of metal foam by different methods: a review, Mater. Today 26 (2020) 1784–1790, https://doi.org/10.1016/j.matpr.2020.02.375, 2020/01/01/.

[32] W.Q. Li, Z.G. Qu, Y.L. He, Y.B. Tao, Experimental study of a passive thermal management system for high-powered lithium ion batteries using porous metal foam saturated with phase change materials, J. Power Sources 255 (2014) 9–15, https://doi.org/10.1016/j.jpowsour.2014.01.006, 2014/06/01/.

[33] P. Zhang, Z.N. Meng, H. Zhu, Y.L. Wang, S.P. Peng, Melting heat transfer characteristics of a composite phase change material fabricated by paraffin and metal foam, Appl. Energ. 185 (2017) 1971–1983, https://doi.org/10.1016/j.apenergy.2015.10.075, 2017/01/01/.

[34] S. Mancin, A. Diani, L. Doretti, K. Hooman, L. Rossetto, Experimental analysis of phase change phenomenon of paraffin waxes embedded in copper foams, Int. J. Therm. Sci. 90 (2015) 79–89, https://doi.org/10.1016/j.ijthermalsci.2014.11.023, 2015/04/01/.

[35] H. Liu, S. Ahmad, Y. Shi, J. Zhao, A parametric study of a hybrid battery thermal management system that couples PCM/copper foam composite with helical liquid channel cooling, Energy 231 (2021) 120869, https://doi.org/10.1016/j.energy.2021.120869, 2021/09/15/.
[36] M.S. Isfahani, A. Gharehghani, S. Saeedipour, M. Rabiei, PCM/metal foam and microchannels hybrid thermal management system for cooling of Li-ion battery, J. Energy Storage 72 (2023) 108789, https://doi.org/10.1016/j.est.2023.108789, 2023/11/30/.
[37] Z. Sun, et al., Experimental study of battery passive thermal management system using copper foam-based phase change materials, Int. J. Thermofluids 17 (2023) 100255, https://doi.org/10.1016/j.ijft.2022.100255, 2023/02/01/.
[38] X. Liu, F. Yang, M. Li, C. Sun, Y. Wu, Development of cost-effective PCM-carbon foam composites for thermal energy storage, Energy Rep. 8 (2022) 1696–1703, https://doi.org/10.1016/j.egyr.2021.12.065, 2022/11/01/.
[39] J. Shi, H. Du, Z. Chen, S. Lei, Review of phase change heat transfer enhancement by metal foam, Appl. Therm. Eng. 219 (2023) 119427, https://doi.org/10.1016/j.applthermaleng.2022.119427, 2023/01/25/.
[40] N. Bianco, S. Busiello, M. Iasiello, G.M. Mauro, Finned heat sinks with phase change materials and metal foams: Pareto optimization to address cost and operation time, Appl. Therm. Eng. 197 (2021) 117436, https://doi.org/10.1016/j.applthermaleng.2021.117436, 2021/10/01/.
[41] H. Zhang, et al., Polyurethane foam with high-efficiency flame retardant, heat insulation, and sound absorption modified by phosphorus-containing graphene oxide, ACS Appl. Polym. Mater. 6 (3) (2024) 1878–1890, https://doi.org/10.1021/acsapm.3c02706, 2024/02/09.
[42] L.W. Sommer, et al., Embedded fiber optic sensing for accurate state estimation in advanced battery management systems, Mrs Proc. 1681 (2014), https://doi.org/10.1557/opl.2014.560.
[43] S. Inazawa, A. Hosoe, M. Majima, K. Nitta, Novel plating technology for metallic foam, SEI Tech. Rev. 71 (2010) 23–30.
[44] H. Yang, Y. Bai, C. Ge, C. Ma, W. Liang, X. Zhang, Modified melamine foam-based flexible phase change composites: enhanced photothermal conversion and shape memory properties, ACS Appl. Polym. Mater. 3 (7) (2021) 3321–3333, https://doi.org/10.1021/acsapm.1c00184, 2021/07/09.
[45] K. Ankang, H. Houde, Effective thermal conductivity of open cell polyurethane foam based on the fractal theory, Adv. Mater. Sci. Eng. 2013 (2013) 125267, https://doi.org/10.1155/2013/125267, 2013/12/09.
[46] L. Wang, L. Sun, J. Li, Electroless copper plating on Fraxinus Mandshurica veneer using glyoxilic acid as a reducing agent, Biosources 6 (3) (2011) 3493–3504.
[47] W. Sha, X. Wu, K.G. Keong, Electroless Copper and Nickel-Phosphorus Plating: Processing, Characterisation and Modelling, Woodhead Publishing, 2011.
[48] F. Hanna, Z.A. Hamid, A.A. Aal, Controlling factors affecting the stability and rate of electroless copper plating, Mater. Lett. 58 (1–2) (2004) 104–109, https://doi.org/10.1016/s0167-577x(03)00424-5.
[49] M. Schlesinger, M. Paunovic, Modern Electroplating, 5th ed., John Wiley & Sons, 2014.
[50] H. Lan, et al., Graphite foam infiltration with mixed chloride salts as PCM for high-temperature latent heat storage applications, Sol. Energy 209 (2020) 505–514, https://doi.org/10.1016/j.solener.2020.09.029, 2020/10/01/.
[51] T. Nomura, N. Okinaka, T. Akiyama, Impregnation of porous material with phase change material for thermal energy storage, Mater. Chem. Phys. 115 (2) (2009) 846–850, https://doi.org/10.1016/j.matchemphys.2009.02.045, 2009/06/15/.
[52] B. Shang, J. Hu, R. Hu, J. Cheng, X. Luo, Modularized thermal storage unit of metal foam/paraffin composite, Int. J. Heat Mass Transf. 125 (2018) 596–603, https://doi.org/10.1016/j.ijheatmasstransfer.2018.04.117, 2018/10/01/.